

Pres. at Denver '96
Denver, CO, 4-9 August (1996)

BNL-62825

CONF-960848--24

SIGNIFICANT IMPROVEMENTS IN LONG TRACE
PROFILER MEASUREMENT PERFORMANCE*

Peter Z. Takacs
Brookhaven National Laboratory
Upton, NY 11973-5000

Cynthia J. Bresloff
Argonne National Laboratory
Argonne, IL 60439

RECEIVED
SEP 11 1996
OSTI

July, 1996

MASTER

*This research was supported by the U. S. Department of Energy under Contract No. DE-AC02-76CH00016.

HH
DISTRIBUTION OF THIS DOCUMENT IS UNLIMITED

Significant Improvements in Long Trace Profiler Measurement Performance

Peter Z. Takacs

Brookhaven National Laboratory
Upton, New York 11978-5000

Cynthia J. Bresloff*

Argonne National Laboratory
Argonne, IL 60439

ABSTRACT

Modifications made to the Long Trace Profiler (LTP II) system at the Advanced Photon Source at Argonne National Laboratory have significantly improved the accuracy and repeatability of the instrument. The use of a Dove prism in the reference beam path corrects for phasing problems between mechanical errors and thermally-induced system errors. A single reference correction now completely removes both error signals from the measured surface profile. The addition of a precision air conditioner keeps the temperature in the metrology enclosure constant to within $\pm 0.1^\circ\text{C}$ over a 24 hour period and has significantly improved the stability and repeatability of the system. We illustrate the performance improvements with several sets of measurements. The improved environmental control has reduced thermal drift error to about 0.75 microradian RMS over a 7.5 hour time period. Measurements made in the forward scan direction and the reverse scan direction differ by only about 0.5 microradian RMS over a 500mm trace length. We are now able to put 1-sigma error bar of 0.3 microradian on an average of 10 slope profile measurements over a 500mm long trace length, and we are now able to put a 0.2 microradian error bar on an average of 10 measurements over a 200mm trace length. The corresponding 1-sigma height error bar for this measurement is 1.1 nm.

Keywords: Profilometry, surface metrology, optical metrology, figure measurement

1. Introduction

The Long Trace Profiler (LTP), originally developed at Brookhaven National Laboratory (BNL), is a scanning pencil beam interferometer system that is optimized for measuring the figure and slope errors on cylindrical aspheres.¹⁻⁴ Its primary use is to measure mirrors to be used in synchrotron radiation (SR) beam lines at the various synchrotron facilities around the world. It can also be used to measure x-ray telescope mirrors oriented in a vertical configuration, so as to minimize errors caused by self-weight deflections.⁵ The current version of the LTP, the LTP II, was developed under the auspices of a Cooperative Research and Development Agreement (CRADA) between Continental Optical Corporation and BNL, and in collaboration with Lawrence Berkeley Laboratory.

The optical diagram in Fig. 1 shows the basic configuration of the LTP II optical system. A HeNe laser beam from a collimated fiber optic source is split into two beams by an arrangement of a cube beam splitter and two right angle prisms. The resultant parallel and collinear beam pair is adjusted so that the separation distance between each beam is about 1 mm. The beam pair passes through another cube beam splitter and is divided into a test beam and a reference beam. The test beam propagates down to a test surface and is scanned across the surface as the optical head moves along an air bearing slide. The reflected beam returns back into the optical head and is focused onto a linear array detector. The two components of the test beam pair form an interference pattern on the detector, similar to Young's fringes within the Airy disk of the laser beam focal spot. The position of the minimum in the focal spot is directly related to the local slope of the surface under test. Likewise, the other beam pair is reflected from a reference mirror and forms another focal spot on the detector.⁶

The nominal position of the laser beams on the reference mirror does not change as the optical head is scanned. Any deviation from a fixed location on the detector is a measure of the tilt error in the mechanical system during the scanning motion. This error is also present in the SUT signal and can be removed simply by subtracting the reference signal from the test signal. The resultant corrected signal is an absolute measure of the slope profile of the surface. The height profile can be generated by simple integration of the slope profile.

DISCLAIMER

This report was prepared as an account of work sponsored by an agency of the United States Government. Neither the United States Government nor any agency thereof, nor any of their employees, makes any warranty, express or implied, or assumes any legal liability or responsibility for the accuracy, completeness, or usefulness of any information, apparatus, product, or process disclosed, or represents that its use would not infringe privately owned rights. Reference herein to any specific commercial product, process, or service by trade name, trademark, manufacturer, or otherwise does not necessarily constitute or imply its endorsement, recommendation, or favoring by the United States Government or any agency thereof. The views and opinions of authors expressed herein do not necessarily state or reflect those of the United States Government or any agency thereof.

DISCLAIMER

Portions of this document may be illegible in electronic image products. Images are produced from the best available original document.

The error correction algorithm works well when the LTP II is located in a stable thermal environment. For truly repeatable measurements, we estimate that the temperature must be maintained to better than ± 0.01 C over several hours. In most installations, this kind of temperature control is not possible. This prompted us to examine the nature of the error sources and make a simple change to the optical system that has relaxed the thermal stability requirement and improved the system performance significantly.

2. Error sources

The major error source in any LTP measurement is produced by pitch errors of the optical head as it moves along the air bearing slide. Fig. 2 illustrates the origin of the mechanically-induced error signal. The test mirror and reference mirror are stationary in the laboratory frame. The normal location of the images from both the test and reference arms is along the O-axis in the unrotated optical head. When the optical head rotates by a small error angle, α , the two beams are deflected to opposite sides of the original optical axis, which is now also rotated by the angle α . The net result is that the reference beam error signal is "out-of-phase" with respect to the test signal. In order to correct for the error, the reference signal must be added to the test signal. The reason for this is seen by counting and comparing the number of reflections made by each beam after exiting the optical head (the region enclosed by the solid and dotted lines). If the difference in the number of reflections between each arm is an odd number, then the correction is an addition; if the difference is an even number, the correction is a subtraction. In the case of mechanical pitch errors caused by the translation of the optical head along the air bearing, the difference is an odd number and the correction is an addition, as noted earlier.

Not all error sources produce out-of-phase error signals. If the pointing direction of the laser beam rotates by a small angle, tracing the beam path through the unrotated optical system indicates that beams in both arms rotate by the same angle in the same direction. This "in-phase" error is opposite to the mechanically-induced "out-of-phase" error. There are a number of possible sources for the "in-phase" error, one of which is a change in the optical path between the two components of each probe beam pair. The source of this error is most likely a thermal drift between the two supports for the right angle prisms, which causes the optical path difference between them to change by several nanometers. The resultant shift in the fringe position for this error is on the order of several microradians, which is relatively large when one is trying to measure actual surface errors on the order of 1 microradian. The real problem with the present LTP optical system is that if we correct for one error source, we double the other error. We can eliminate the mechanical errors by adding the test and reference beam signal, but, by doing so, we double the thermal errors. In the past, we have performed the correction to eliminate the mechanically-induced errors, since they are typically much larger than the thermal errors. However, as the need for more accurate and repeatable measurements grows, we must deal with both error sources.

3. Error correction with Dove prism

Fortunately, there is a simple solution to the problem. By adding a Dove prism into the reference beam, attached to the optical head, we effectively increase the number of reflections in the reference arm path by one for mechanical errors and by two for thermal errors. The net result is that BOTH error sources are now "in-phase", and both errors can be corrected by simply subtracting the reference beam from the test beam. Figure 3 illustrates the path of the beams through the Dove prism system for a mechanical rotation of the optical head. Both beams are deflected to the same side of the original beam position by the same angle. Analysis of each individual beam pair shows that the phase shift within each pair is also "in-phase" at the detector. So a simple algebraic subtraction removes both error sources.

4. Stability scan results

The success of the Dove prism error correction method is illustrated by a number of examples. The results of a "stability" scan over a 7.5 hour time period are shown in Fig. 4. The carriage remains stationary during a stability scan, but the detector records data as if it were a normal scan. In this case, a data point was recorded once every 30 seconds during an overnight measurement run. The uncorrected test and reference beams are displayed separately to show that the combined error sources produce a total change of about 30 microradians in each beam, but the difference between them is only 0.75 microradians RMS. The most striking feature of this data set is the 6.5 minute periodicity in each signal caused by the inherent ± 0.1 C limit cycle in the precision air conditioner. This temperature fluctuation produces a modulation with an amplitude of about 4 microradians in each signal. The correction process, however, completely removes both the long term drift and the short term fluctuations, and the resultant difference is absolutely flat with a very small residual RMS value.

Another example of the quality the error correction during a short stability scan is shown in Fig. 5. Data points were taken at 1 second intervals to simulate a typical scan time on a 100mm long surface. During the scan, external force was applied to the air bearing carriage several times by hand to simulate the pitch errors introduced during the carriage motion. Again, the individual test and reference arm signals are shown, displaced from each other by 5 microradians for better visibility. One can see that they track each other almost exactly. The difference between them is also shown, using the 5-times magnified scale on the right side. One can see that the correction for mechanically-induced errors is also nearly perfect. The glitches apparent in the last force application are probably caused by the suddenness of the large force applied and the sequential nature of the dual array detector readout. The reference beam is centered on one row of the detector, while the test beam is positioned on the other row. Any difference in applied force between the readout times of the two rows will show up as a slight shift in one of the fringe patterns, and the correction will not be complete. The net result of the tests shown in Figures 4 and 5 indicate that both the thermal and mechanical errors are completely corrected through the use of the Dove prism in the optical system.

5. Repeatability measurements

The improved thermal stability and error correction afforded by the Dove prism system has resulted in a significant improvement in measurement accuracy and repeatability. Repeatability is illustrated by a series of ten measurements made on a 500mm long nominally "flat" surface. The individual scans are shown superimposed in Fig. 6. Each has had only the mean removed. From this set, we can generate the mean slope profile by simply averaging all 10 and then subtract the mean profile from each individual to generate a set of residuals. The residuals are a measure of the system noise level. From the residuals, we can estimate the RMS error in each data point, in each profile, and in the mean profile. The result of this process for the estimate of the one-standard-deviation-in-the-mean error bar is $1\sigma = 0.29\ \mu\text{rad}$. This error bar is shown on the detrend 1 slope profile in Fig. 7, which is generated by subtracting a least-squares-fit 1st order polynomial from the mean slope profile. This curve with no error bars is plotted offset below it to show more clearly the significance of small features that are of the same magnitude as the error bar.

Another example of improved repeatability is illustrated in Fig. 8. This plot compares the results of two separate scans made on the same surface, but in opposite directions. One scan was made scanning from left-to-right; the other was made scanning right-to-left. The forces transmitted to the carriage and into the optical head by the drive motor and the cable carrier attached to the back of the carriage are very different in the two drive directions. Prior to the use of the Dove prism, we have always noted significant differences in measured profiles cause by this systematic error source. Fig. 8 shows that this error source has effectively been eliminated with the Dove prism system. The difference between the forward and reverse scans is nearly the same as for a stability scan, which indicates that each scan is essentially identical. There is no difference between scans made in the forward direction and in the reverse direction.

A final example of the repeatability of the system is illustrated by a series of measurements on an extreme long-radius spherical surface. A set of 10 scans was made along a diameter of a fused silica disk. Each scan consisted of 200 points at 1 mm intervals. The standard-deviation-in-the-mean for the average slope profile is $0.21\ \mu\text{rad}$. Integration of the mean slope profile results in the height profile shown in Fig. 9. The radius of curvature for this surface is 5.5 km. The $1\text{-}\sigma$ error bar for this height profile, generated by looking at the statistics of each individual height profile, is 1.09 nm RMS. The size of this error bar is about the same as the thickness of the line in Fig. 9, so we remove the overall curvature from the profile and show the detrend 2 height profile in Fig. 10. Now one can see the significance of the surface features in light of the magnitude of the error bar. The detrend 2 profile exhibits a strong 4th order residual component. After removing this 4th order term, the detrend 4 residual profile has an RMS value of 1.11 nm, which is essentially at the level of the system noise for this measurement.

6. Summary

The addition of the Dove prism to the optical system of the LTP II and the use of a precision air conditioner to maintain thermal stability over long time periods have significantly improved measurement reliability and repeatability. Both mechanical and thermal errors are completely corrected by simple algebraic subtraction of the test and reference signals. Removal of these major error sources will enable us to investigate less significant errors that have been masked by the two larger sources. Imperfections in system alignment and in the internal optical system parts can now be seen that produce recognizable effects at the microradian and sub-microradian levels. These effects are now easily accessible to measurement.

7. Acknowledgment

This research was supported by the U.S. Department of Energy: Contract No. DE-AC02-76CH00016.

8. References

1. K. von Bieren, "Pencil Beam Interferometer for Aspherical Optical Surfaces," Proc. SPIE 343, 101 (1982)
2. K. von Bieren, "Interferometry of Wavefronts Reflected Off Conical Surfaces," Appl. Opt. 22, 2109, (1983)
3. P.Z. Takacs, S.-C.K. Feng, E.L. Church, S.-N. Qian, and W.-M. Liu, "Long trace profile measurements on cylindrical aspheres," in *Advances in Fabrication and Metrology for Optics and Large Optics*, Jones B. Arnold and Robert A. Parks, eds., Proc. SPIE 966, 354-364 (1989).
4. P.Z. Takacs, K. Furenlid, R. DeBiasse, and E.L. Church, "Surface topography measurements over the 1 meter to 10 micrometer spatial period bandwidth," in *Surface Characterization and Testing II*, J.E Grievenkamp and M. Young, eds., Proc. SPIE 1164, 203-211 (1989).
5. H. Li, X. Li, M.W. Grindel, and P.Z. Takacs, "Measurement of X-ray Telescope Mirrors Using A Vertical Scanning Long Trace Profiler," Opt. Eng. 35 (2), 330-338, (1996).
6. S.C. Irick, W.R. McKinney, D.L.T. Lunt, and P.Z. Takacs, "Using a straightness reference in obtaining more accurate surface profiles", Rev. Sci. Instrs., Vol. 63, 1436-1438, (1992).

*Current address: Tinsley Laboratories, Inc., 3900 Lakeside Drive, Richmond, CA 94806

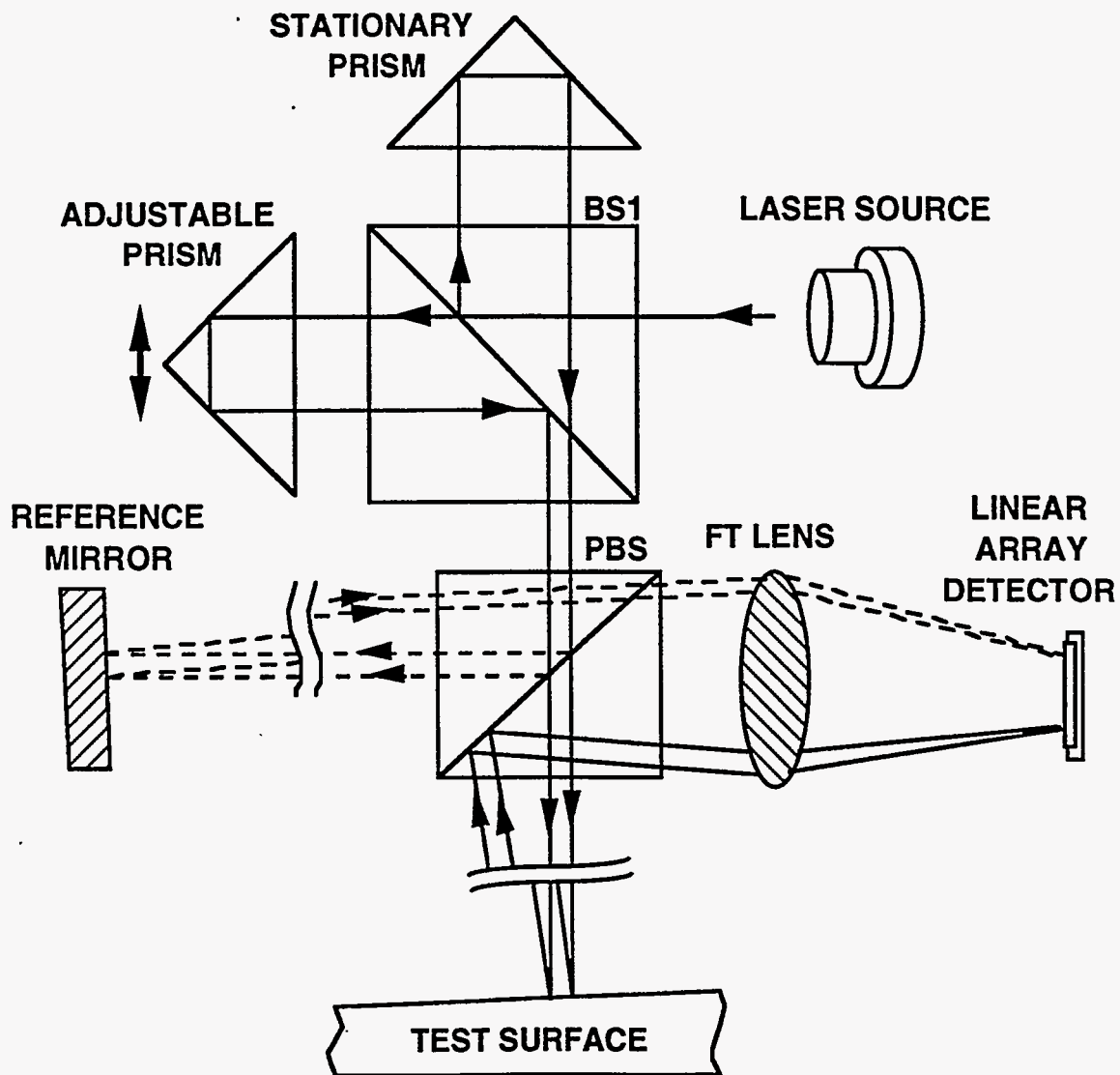


Fig. 1 - Schematic diagram of the standard LTP II optical system. The first beam splitter, BS1, and the right-angle prisms separate the laser beam into two collinear beams. The polarizing beamsplitter, PBS, separates them further into two pairs of beams, which are directed to a test surface or the reference mirror. The return beams each form a separate interference pattern on the detector.

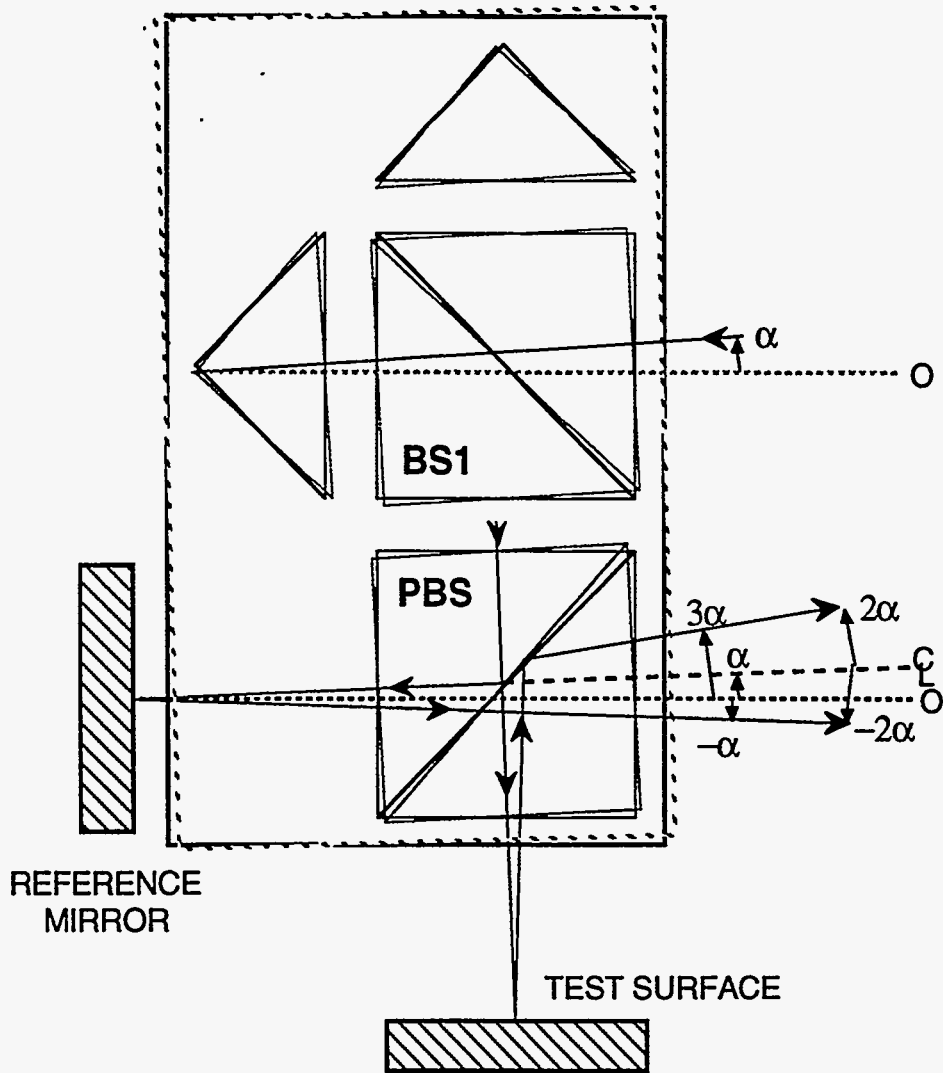


Fig. 2 - Path of laser beam pairs in standard LTP II for an optical head pitch angle error $+\alpha$ clockwise relative to the laboratory coordinate system (indicated by "O"). The center line of the original beam direction rotates by $+\alpha$ relative to "O", but the two return beams rotate by an equal but opposite angle, $\pm 2\alpha$, about the original beam center line. The detector sees a shift in each by 2α , but in opposite directions. The error is "out of phase".

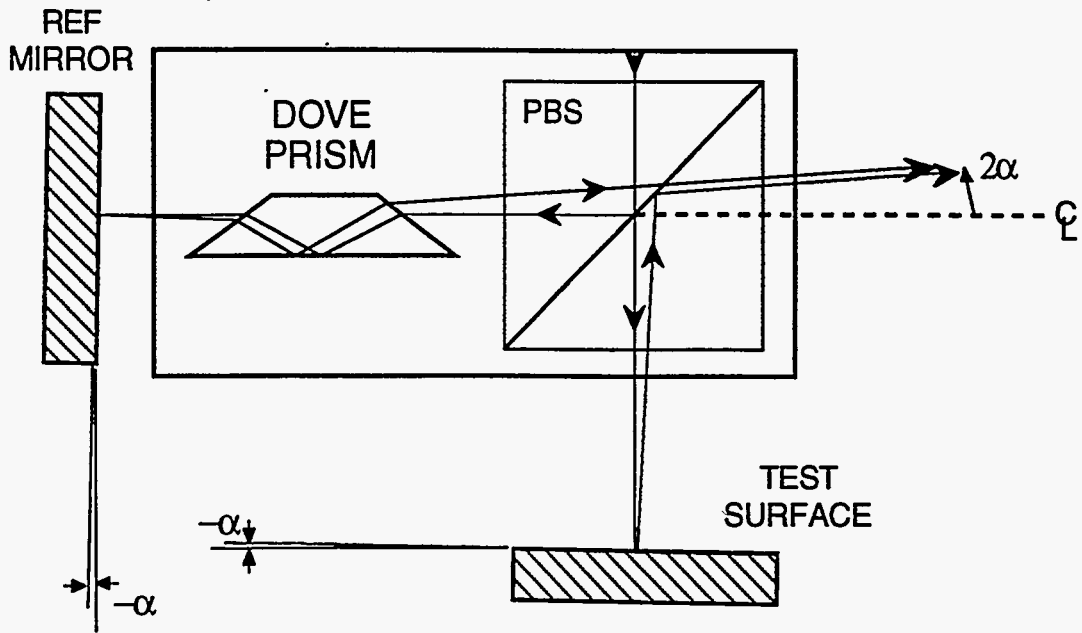


Fig. 3 - Optical path for laser beams in the modified LTP II optical head with the addition of a Dove prism fixed to the optics board. Both beam deflection errors are now "in phase" on the same side of the original center line.

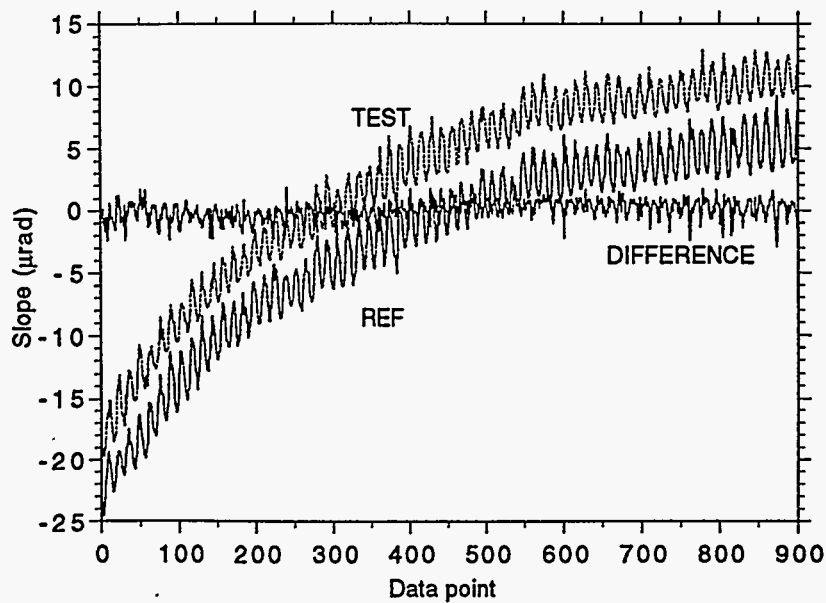


Fig. 4 - Stability scan run overnight for 7.5 hours at 30 second per point. Total drift in test and reference beams is about 30 μrad , but the difference is only 0.75 μrad RMS. The 6.5 minute period is related to the $\pm 0.1\text{C}$ air conditioner cycle time.

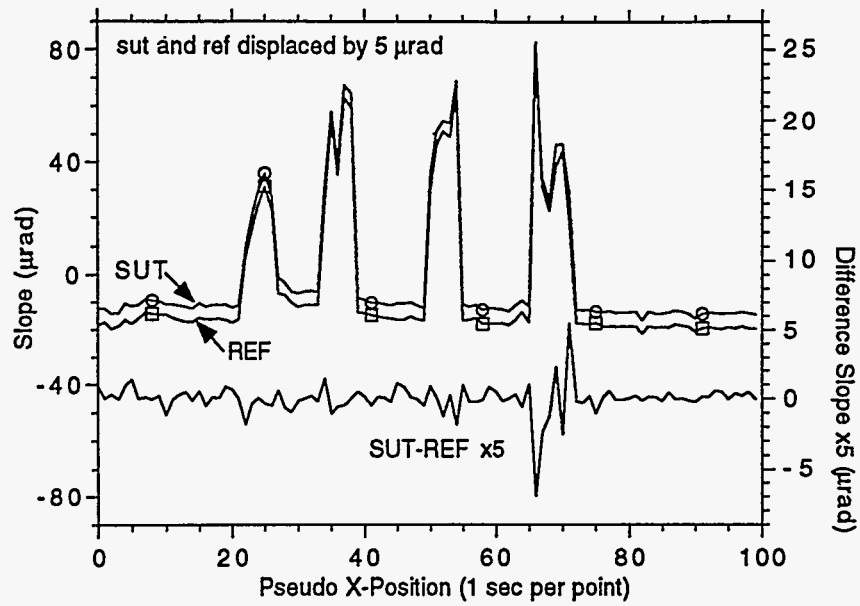


Fig. 5 - Error cancellation test from a stability scan using a Dove prism with external force applied to the optical head by hand. Carriage is stationary while data is recorded at the normal scan rate. Two upper curves (left side scale) are the raw slope signals for the test and reference beams, displaced slightly for clarity. Bottom curve (right side scale) is the difference magnified by 5 times in the vertical. Error cancellation is nearly complete.

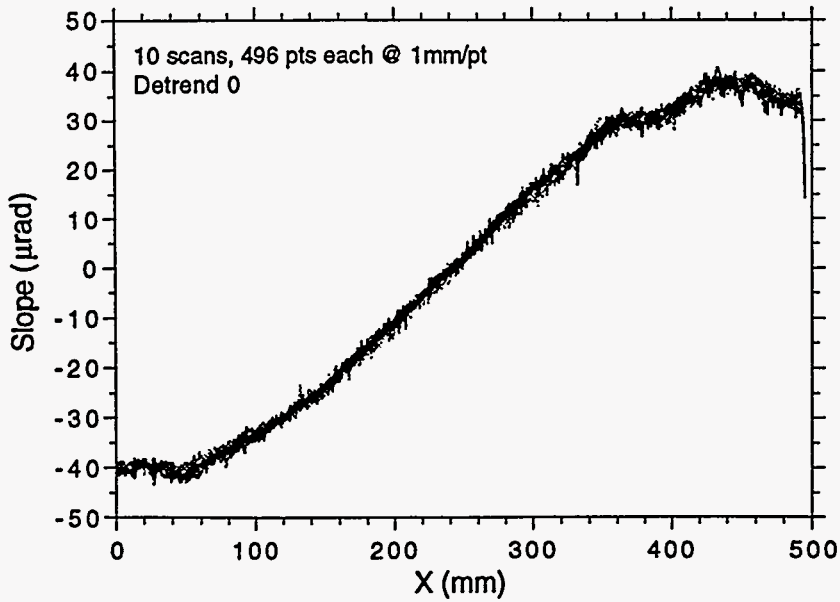


Fig. 6 - Repeatability test with slope profiles from 10 scans, each 496 points at 1 mm per point. Only the mean has been removed from each (detrend 0).

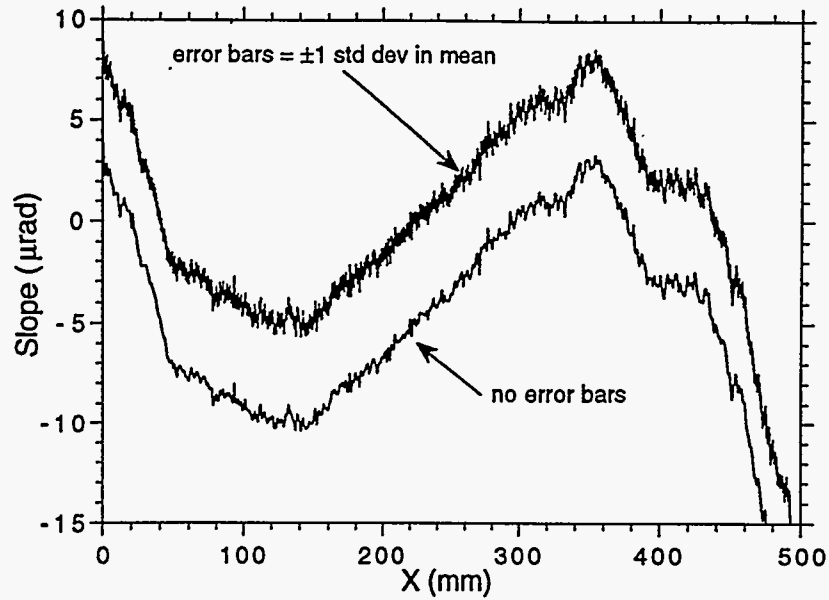


Fig. 7 - Detrend 1 of average slope profile from Fig. 6 data shows the residual surface slope error. Lower curve shown without error bars. Upper curve shown with $\pm 1 \sigma = \pm 0.29 \mu\text{rad}$ error bars. Significance of features observed in the profile can be related to the magnitude of the error bar. RMS slope error for the detrend 1 profile is $4.88 \mu\text{rad}$.

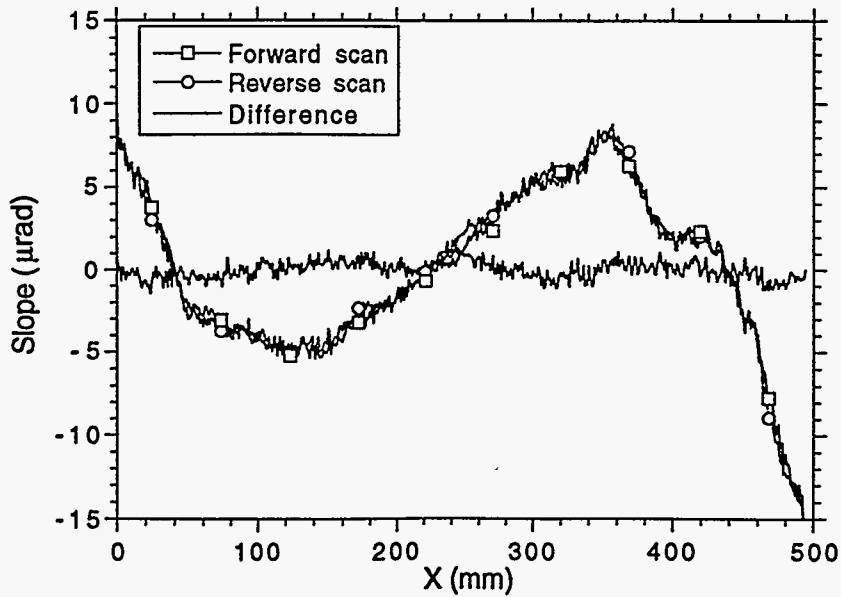


Fig. 8 - Comparison of forward and reverse scans. The residual slope profiles of the detrend 1 forward and reverse average scans are nearly identical. The difference between the two is shown as the horizontal line about the mean of zero. The RMS of the difference is $0.51 \mu\text{rad}$.

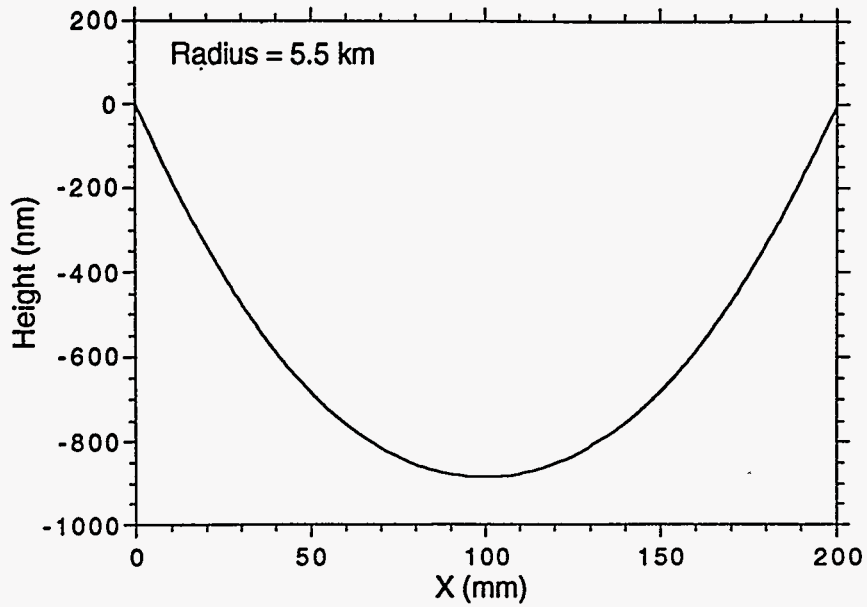


Fig. 9 - The average detrend 0 height profile for the fused silica disk. The error bar size is about the same as the line width on this vertical scale.

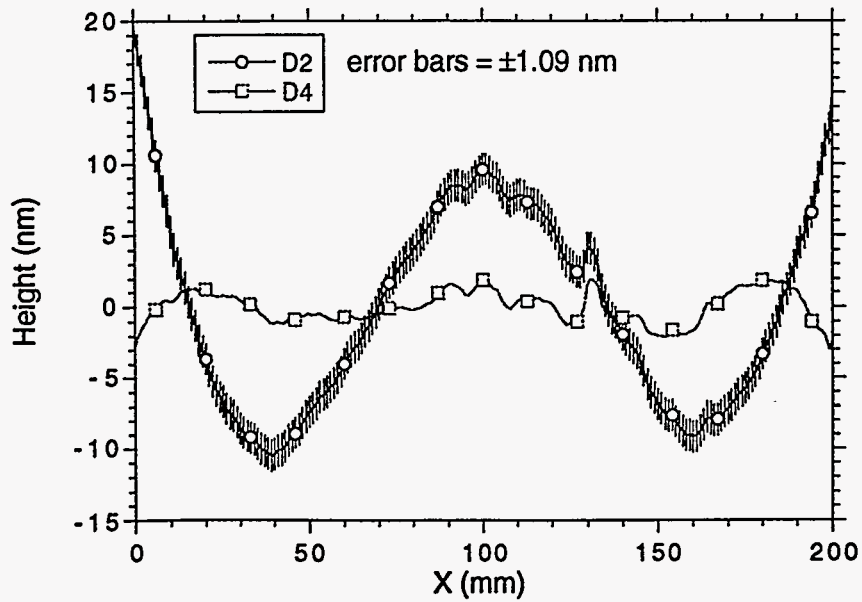


Fig. 10 - Residual height profiles of the fused silica disk after removing a 2nd order fit (D2 shown with error bars) and a 4th order fit (D4). The error bars allow one to assess what features on the surface are real. The RMS computed for the 4th order curve is 1.11 nm, which is effectively at the noise level of the instrument in this case.